Chiang Mai J. Sci. 2019; 46(6) : 1249-1255
http://epg.science.cmu.ac.th/ejournal/
Contributed Paper

Gamma Irradiation on Rubellite Tourmaline

Nantharat Bunnag*[a] and Tasnara Sripoonjan [b]

[a] Integrated & Innovative Jewelry Materials Research Unit, Faculty of Gems, Burapha University (Chanthaburi Campus): 57 M.1 Ka-Mong, Thamai, Chanthaburi, 22120, Thailand.

[b] The Gem and Jewelry Institute of Thailand (Public Organization): 4th Floor, ITF Tower. Silom Rd., Bangrak, Bangkok, 10500, Thailand.

*Author for correspondence; e-mail: b_nantharat@yahoo.com

Received: 10 June 2019
Revised: 25 July 2019
Accepted: 1 August 2019

ABSTRACT

Effect of gamma rays on changes color of rubellite tourmaline from Afghanistan, Mozambique and Nigeria were studied. The gamma irradiation process was done using cobalt-60 radiation; the samples were irradiated to 100 Mrad. Most samples had their color changed. It was obviously seen in the Afghanistan samples. Their optical spectra were investigated by UV-Vis spectroscopy. After irradiation, most samples showed stronger absorption band of Mn^{3+}, centered at 520 nm. Additionally, the irradiated Mozambique and Nigeria samples became darker brown tint related with an increasing of Fe^{2+}-Ti^{4+} IVCT absorption band. The trace elements analysis proved that the Afghanistan samples contained higher manganese than the samples from Mozambique and Nigeria. In the other hand, the iron content of Afghanistan samples were much lower than that of Mozambique and Nigeria samples.

Keywords: tourmaline, rubellite, gamma irradiation, optical absorption

1. INTRODUCTION

Tourmaline is a well-known gemstone in gem trade as the most various color gemstone. As one of boro-silicate minerals, tourmaline has a very complex and variable chemical compositions. The ideal chemical formula can be written as $XY_3Z_6(BO_3)_3Si_6O_{18}(OH, O)_3(OH,F)$ where X is Na^+, Ca^{2+} or vacancies, sometimes Mg^{2+}, Fe^{2+} or Mn^{2+}, and Y is normally Al^{3+}. However, Y may be substituted by ion of other transition metals (Fe, Mn, Cr, Ti, Zn) as well as Li and Mg. The Z site is in general occupied by Al^{3+}. The basic structural units are hexagonal rings of Si_6O_{18} that form basal planes and are connected with Na, Li and Al octahedra and distorted BO_3 groups. Two oxygen-related sites have to be distinguished: the O_1 site lies in the center of the silicate ring on the three- fold axis and is substituted to some percentage by F or OH. The O_3 site is located at the border of the rings and contains either oxygen or OH depending on the charge compensation of the cationic sites [1].

One of the valuable tourmaline varieties is rubellite whose color ranges from strong pink, purplish pink to purplish red color. Vivid pinkish red to purplish red without brownish tones are the most desirable colors. Fine rubellite comes from Brazil. There are also other pink colors which are so called pink tourmaline. They are extracted in Brazil, Afghanistan, Kenya, Tanzania, Madagascar, Malawi and Mozambique. Causes of the pink and red color in tourmaline are Mn^{2+} and Mn^{3+}. The pink color can be generally improved by gamma irradiation [2] and electron beam irradiation [3]. The gamma irradiation uses lower energy than that of the electron beam then there is less radio nuclei. Other tourmaline colors can be enhanced by heat treatment. However, heat treatment is not suitable for pink tourmaline because it is changed to colorless when heating [3].

Nowadays, pink tourmaline are mostly from Afghanistan, Nigeria and Mozambique. To increase the value of the gems in the market, the samples from these localities were selected to study the opportunity of color enhancement by gamma irradiation.

2. MATERIALS AND METHODS

Twelve samples of pink tourmaline from Afghanistan, Mozambique and Nigeria were investigated, four samples from each country. The Afghanistan samples were light pink while Mozambique samples were light pink with brownish tint and Nigeria sample were slightly purplish red. Samples were prepared by cutting and polishing in to two pairs of parallel planes which were paralleled to c-axis (//c) and one pair of parallel planes which were perpendicular to c-axis (⊥c).

The tourmaline samples were separated into two batches for two different irradiation. Batch 1 composed of the sample number 01 and 02 and batch 2 composed of the sample number 03 and 04. The samples in batch 1 and batch 2 were irradiated up to 100 Mrad and 200 Mrad, respectively. Change of the colors were observed by naked eyes (Table 1) and determined by CIE L*a*b* color index (Table 2) on the plane parallel to c-axis (//c).

Optical spectra and CIE L*a*b* color index were collected both on the planes parallel to c-axis (//c) and perpendicular to c-axis (⊥c) by using Hitachi U4100, UV-Vis-NIR spectrophotometer at 2 nm resolution, scan speed 300 nm/min. The total color difference (ΔE*) was calculated as shown in Table 2 [$\Delta E^* = (\Delta L^{*2} + \Delta a^{*2} + \Delta b^{*2})^{1/2}$] where +L* is the lightness; -L* is the darkness +a* is red; - a* is green; +b* is yellow and -b* is blue. The trace elements concentration was analyzed by LA-ICP-MS, New Wave Research UP213 laser ablation equipped with Agilent 7500CS Inductively Coupled Plasma Mass Spectrometry System. The NIST SRM 610 glass was used as standard. The analysis duration was 153 seconds (65 seconds background, 88 seconds signal) by 55 μm diameter nominal spot size.

3. RESULTS AND DISCUSSIONS

After irradiation, color of the Afghanistan samples was changed from pink to red color. The plotting of a* versus b* color index of Afghanistan samples located in red-blue quadrant (a*, red increasing) as shown in Figure 1, while that most of Mozambique and Nigeria samples were in red-yellow quadrant as shown in Figure 2 and Figure 3, respectively. The color of Mozambique samples changed from pink with brownish color zoning to slightly darker yellowish -brownish tint (Table 1) as the L* was decreased. The a* values of the samples were slightly decreased while b* values were slightly increased (Figure 2). The Nigeria samples had slightly darker color in both body color and color zoning (Table 1 and Figure 3). In comparison of the total color difference (ΔE*) between the 100 and 200 Mrad irradiation intensity, most samples irradiated by 200 Mrad showed more obvious change of color than that of 100 Mrad.

Optical spectra of the pink-red samples showed absorption bands related to Mn^{2+} and Mn^{3+}. Mn^{2+} feature is easily recognized by their

Table 1 Samples' color before and after irradiation.

Sample	Before Irradiation	After Irradiation	Absorbed Dose
Af_01			100 Mrad
	Sample dimension 4.11 x 8.25 x 2.12 mm		
Af_02			100 Mrad
	Sample dimension 2.41 x 7.17 x 2.40 mm		
Af_03			200 Mrad
	Sample dimension 5.02 x 7.42 x 3.34 mm		
Af_04			200 Mrad
	Sample dimension 4.86 x 7.29 x 3.72 mm		
Mo_01			100 Mrad
	Sample dimension 4.54 x 6.93 x 2.33 mm		
Mo_02			100 Mrad
	Sample dimension 4.34 x 7.51 x 2.63 mm		
Mo_03			200 Mrad
	Sample dimension 4.11 x 9.42 x 2.00 mm		
Mo_04			200 Mrad
	Sample dimension 4.50 x 10.48 x 2.38 mm		
Ni_01			100 Mrad
	Sample dimension 5.59 x 5.13 x 3.09 mm		
Ni_02			100 Mrad
	Sample dimension 4.49 x 5.70 x 2.35 mm		
Ni_03			200 Mrad
	Sample dimension 4.03 x 6.64 x 1.80 mm		
Ni_04			200 Mrad
	Sample dimension 4.24 x 8.91 x 2.09 mm		

Table 2 The CIE L*a*b* color index of the samples before and after irradiation (measurement on the plane parallel to c-axis (//c)).

Sample	Before Irradiation			After Irradiation			*ΔE**
	*L**	*a**	*b**	*L**	*a**	*b**	
Af_01	49.14	9.14	-3.22	10.30	33.72	-1.70	45.98
Af_02	48.40	8.00	-1.88	12.05	35.11	-2.37	45.35
Af_03	55.01	8.51	-2.56	13.93	41.63	-0.91	52.79
Af_04	61.89	9.54	-2.35	7.87	33.10	-0.65	58.96
Mo_01	46.18	33.47	18.06	27.21	31.37	23.65	19.88
Mo_02	42.25	37.27	11.92	25.53	31.64	16.91	18.34
Mo_03	43.44	38.15	11.57	14.46	25.25	16.17	32.05
Mo_04	39.97	34.50	16.43	15.19	24.17	19.32	27.00
Ni_01	49.41	27.29	10.44	56.09	20.09	5.58	10.96
Ni_02	60.46	13.48	9.61	75.83	16.83	1.41	17.74
Ni_03	48.42	28.86	5.75	31.98	34.12	6.92	17.29
Ni_04	40.55	40.42	-6.51	30.94	40.56	-2.13	10.56

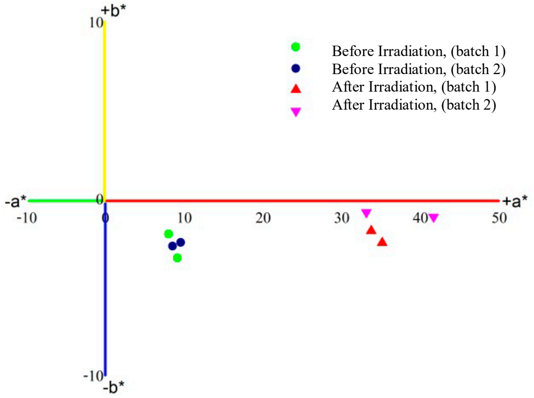

Figure 1. Plotting of a* versus b* color index of Afghanistan samples before and after irradiation.

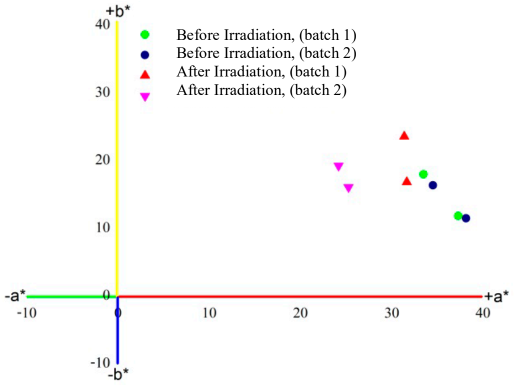

Figure 2. Plotting of a* versus b* color index of Mozambique samples before and after irradiation.

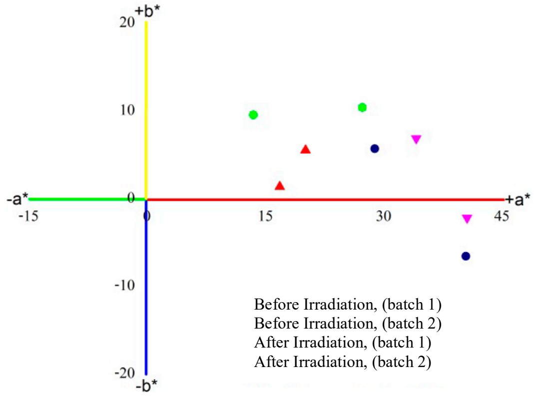

Figure 3. Plotting of a* versus b* color index of Nigeria samples before and after irradiation.

narrow, weak absorption bands between 410 and 420 nm, spin-forbidden Mn^{2+} absorption bands at 414 nm in the E⊥c polarization and at 419, 414, 412 and 408 nm in the E//c polarization [4]. Mn^{3+} absorption band presents at 480 and 700 nm for E//c and at 390, 515 and 700 nm [4,5]. The d^4 configuration of Mn^{3+} ions is assigned to absorption bands at 390 and 513 nm [6]. The weak peaks at 415 and 683 nm could be an attribution from Fe^{2+}-Ti^{4+} intervalence charge transfer (IVCT).

Optical spectra of the untreated Afghanistan sample (Figure 4) showed weak absorption band of Mn^{3+} at 523 nm. After irradiation, the spectrum illustrated full range of Mn^{3+} feature at 390, 515 and 700 nm. The untreated Mozambique sample (Figure 5) showed moderate absorption band of Mn^{3+} at 523 nm, Fe^{2+}-Ti^{4+} intervalence charge transfer (IVCT) at 683 nm and strong absorption edge of UV and visible range. After irradiation, the spectrum indicated higher absorption of Mn^{3+} and Fe^{2+}-Ti^{4+} IVCT. The untreated Nigeria sample (Figure 6) showed absorption of Mn^{3+}, Fe^{2+}-Ti^{4+} IVCT and absorption edge of UV and visible range like the untreated sample from Mozambique. However, after irradiation, the sample displayed the increasing of Mn^{3+} at 523 nm more than other ions.

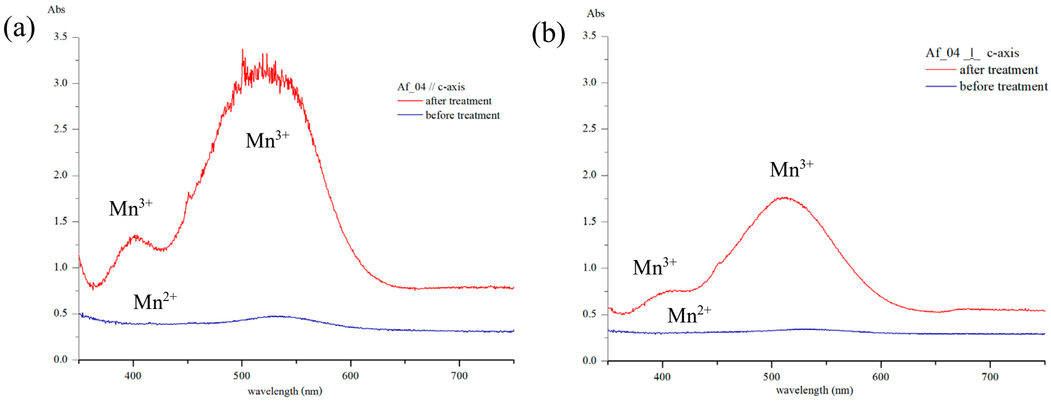

Figure 4. Optical spectra of Afghanistan sample (Af_04), before and after irradiation in (a) //c and (b) ⊥c direction.

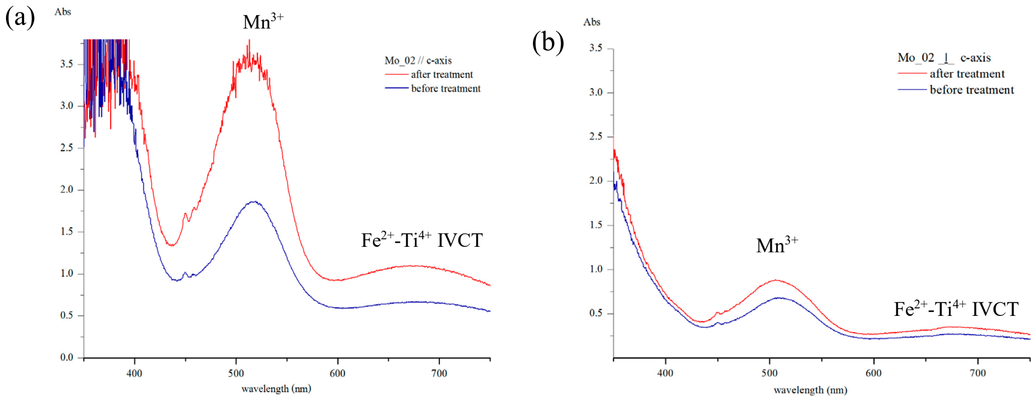

Figure 5 Optical spectra of Mozambique sample (Mo_02), before and after irradiation in (a) //c and (b) ⊥c direction.

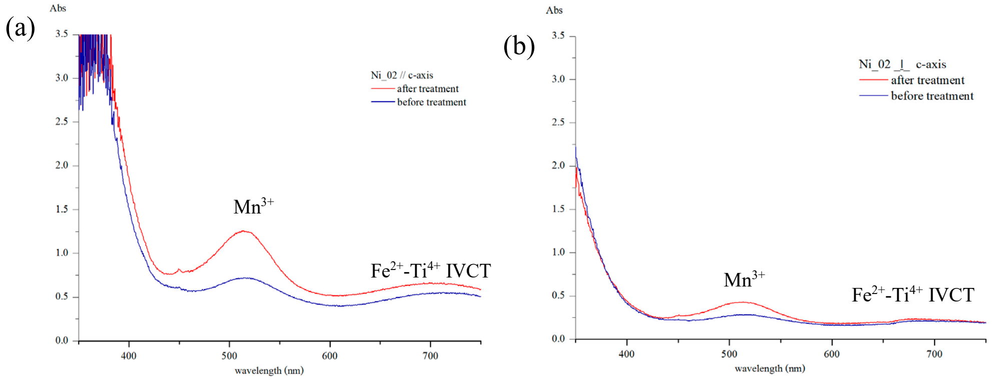

Figure 6 Optical spectra of Nigeria sample (Ni_02), before and after irradiation in (a) //c and (b) ⊥c direction.

The optical absorption behaviors were related to the trace element contents of the samples presented in Table 3. In comparison among three sample localities, the Afghanistan sample contained the highest Mn content without Fe and the related optical absorption clearly showed the complete absorption configuration of Mn^{2+} and Mn^{3+}. The samples with high Mn/Fe ratio showed more intense red color than the one with lower.

The irradiation caused the increse of Mn^{3+} absorption intensity in the samples as shown in their optical spectra. The Af_04 color turned from light pink to strong purplish red. The absorption band was found below 425 nm in both Mozambique and Nigeria contributed to brownish tone. The weak absorption band of Fe^{2+}-Ti^{4+} IVCT centered at 700 nm in Mozambique and Nigeria was slightly increase after the irradiation. Normally, Fe^{2+}-Ti^{4+} IVCT gives green color in tourmaline. However, it promoted brownish tone in pink tourmaline which was clearly observed in Mozambique samples.

Table 3 Trace element concentration of samples (in ppm).

Element	**Sample**		
	Af_04	**Mo_02**	**Ni_02**
Ti	15.66	27.96	43.64
V	0.40	0.31	0.48
Cr	1.17	bdl*	0.68
Mn	3981.43	2958.88	1963.89
Fe	bdl*	535.92	332.96
Co	0.012	bdl*	0.049
Ni	bdl	bdl	bdl
Cu	1.88	0.34	72.01
Mn/Fe	**3981.43**	**5.55**	**5.90**

bdl* : below the detection limit

4. CONCLUSIONS

The color change of pink tourmaline by Gamma irradiation related to the intensity of irradiation and the trace element content in sample. The comparison of optical spectra between before and after irradiation proved that the coloring ions; Mn, Fe and Ti, affected the change of rubellite color. Mn^{3+} was increased after irradiation. The absorption coefficient of intervalence charge transfer (IVCT) was much higher than that of *d-d* transition then the absorption coefficient of Fe^{2+}-Ti^{4+} IVCT was stronger than that of spin–allowed Mn^{3+} (d^4) *d-d* transition which was also stronger than that of spin–forbidden Mn^{2+} (d^5) *d-d* transition. Small content of Fe^{2+}-Ti^{4+} IVCT in tourmaline structure attributed to the absorption band over 620 -800 nm related to the red color absorption. As a result, high intensity of Fe^{2+}-Ti^{4+} IVCT caused the decreasing of red color in irradiated rubellite tourmaline.

ACKNOWLEDGEMENTS

The authors would like to thank Gems Irradiation Center, Thailand Institute of Nuclear Technology (Public Organization) for the contribution on the gamma irradiation process. In addition, for LA-ICP-MS analysis, we are grateful to the Gem and Jewelry Institute of Thailand (Public Organization). Finally, we appreciate the financial support and analytical facilities from Faculty of Gems, Burapha University.

REFERENCES

[1] Krambrock K., Pinheiro M.V.B., Medeiros S.M., Guedes K.J., Schweizer S., Spaeth J.M., *Nucl. Instrum. Meth. B*, 2002; **191**: 241-245. DOI 10.1016/S0168-583X(02)00568-2.

[2] Nassau K., *Gemstone Enhancement*, 2nd Edn., Butterworth-Heinemann, Oxford, 1994.

[3] Maneewong A., Seong B.S., Shin E.J., Kim J.S., Kajornrith V., *J. Korean Phys. Soc.*, 2016; **68** : 83-92. DOI: 10.3938/jkps.68.83

[4] Reinitz I.M., Rossman G.R., *Am. Mineral*, 1988; 73: 822-825.

[5] Chaiyabutr L., Wongkokua W., *J. Mater. Sci. Appl. Energy.*, 2016; 5: 22-25.

[6] Ahn Y., Seo J., Park J., *Vib. Spectrosc.*, 2013; **65**, 165-175. DOI: 10.1016/j.vibspec.2013.01.002